2022 44th Annual International Conference of
the IEEE Engineering in Medicine & Biology Society (EMBC)
Scottish Event Campus, Glasgow, UK, July 11-15, 2022

A Multilayer Monte Carlo Analysis of Optical Interactions in Reflectance Neck Photoplethysmography

Zaibaa Patel[1] and Esther Rodriguez-Villegas[1]

Abstract— **This paper presents a multilayer Monte Carlo model of a healthy human neck to investigate the light-tissue interaction during different perfusion states within its dermal layer. Whilst there is great interest in advancing wearable technologies for medical applications, and non-invasive techniques like photoplethysmography (PPG) have been studied in detail, research has focused on more conventional body regions like the finger, wrist, and ear. Alternatively, the neck could offer access to additional physiological parameters which other body regions are unsuitable for. The aim of this work was to investigate the effects of several factors that would influence the optimum design of a reflectance PPG sensor for the neck. These included the source-detector separation on the optical path, penetration depth, and light detection efficiency. The results were generated from a static multilayer model in a reflectance mode geometry at two wavelengths, 660 nm and 880 nm, containing different blood volume fractions with a fixed oxygen saturation. Simulations indicated that both wavelengths penetrated similar depths, where optimal source-detector separation should not exceed 3 mm or 2.4 mm, for red and infrared respectively. Within this range, light interrogates the dermal-fat boundary corresponding to the last neck tissue layer positively contributing to a neck PPG acquisition.**

I. INTRODUCTION

Wearable sensor technology has advanced over the last decade to enable users to continuously monitor vital cardiovascular and respiratory parameters. Advances in photoplethysmography (PPG) have eased the extraction and monitoring of cardiovascular parameters, such as oxygen saturation (pulse oximetry, PO). The principle PPG/PO is based on light interaction with biological tissues to monitor volumetric changes using an optical sensor, typically consisting of at least two light sources of red and infrared wavelengths and a detector. The detected changes in light intensity are associated with variations in perfusion, which is the blood flow or blood volume per unit tissue mass [1]. PPG remains a desirable physiological sensing technique due to its practical, inexpensive, and non-invasive monitoring capabilities [2].

Whilst manufacturers and researchers are integrating PPG technology into 'consumer-grade' wearables for continuous monitoring, such as watches, earphones and rings, researchers are considering other regions possible for more sophisticated early diagnosis of diseases [2].

The neck is an alternative region of interest, offering greater advantages compared to conventional PPG locations, when it comes to extracting additional biomarkers of interest in the context of respiratory and neurological conditions, which cannot be accurately extracted solely from PPG. For example, in the context of prevention of Sudden Unexpected Death in Epilepsy (SUDEP), the neck could offer the possibility of sensing changes in airflow in combination with drops in oxygen saturation, hence increasing the accuracy in detection of critical physiological events [3].

Previous work demonstrated the feasibility of acquiring neck PPGs characterizing the waveform. However its findings were limited and lacked important information, such as the optimal wearable sensor geometry or the tissue layer the light interrogated [3]. To optimize or miniaturize a wearable sensor design, it is crucial to have an in-depth understanding on the working principle of the technique, specifically for the region of interest [4]. Currently there is no available neck model to determine the wearable sensor design characteristics that would optimize the sensing of neck PPG.

In this work, a neck model based on the Monte Carlo (MC) method was created to understand the optical interactions occurring in the neck's suprasternal notch region. MC modelling computationally simulates photon paths through tissue that are too complex to solve analytically [4]. Such simulations are known to model any sensor geometry and tissue heterogeneity accurately and flexibly [1]. Essential parameters explored included the mean optical pathlength, penetration depth, detection efficiency, and light-tissue interaction profiles at different perfusion states and source-detector separations.

Supported by the European Research Council, grant no. 724334.

[1]Wearable Technologies Lab, Department of Electrical and Electronic Engineering, Imperial College London, SW7 2BT, United Kingdom. E-mail: z.patel@imperial.ac.uk

II. MATERIALS AND METHODS

A. Optical properties and tissue parameters

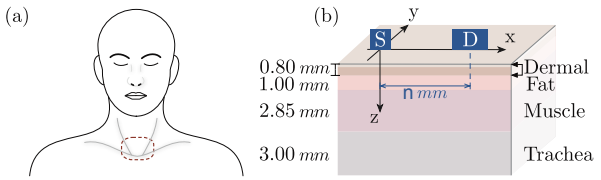

Fig. 1: Illustration of the neck where (a) the suprasternal notch, circled in red, is the ideal location for a wearable sensor, and (b) illustrates the neck tissue layers and thickness. S and D represent the light source and the light detector. Their separation in mm, which varies in the model, is indicated as n.

The neck layers located at the suprasternal notch are the medium of interest for acquiring PPG signals with a wearable technology. The simulated multilayer neck tissue, as shown in Fig 1, consists of 4 layers, where the dermal layer, being the top surface, includes the epidermis. The 3D tissue geometry was considered of infinite length and a thickness of $7.65\,\mathrm{mm}$.

In an optics model utilizing the MC technique, the photon interaction within a medium with absorption and scattering characteristics is simulated. In this case, the suprasternal notch tissue layers constituting the medium are characterized by wavelength dependent optical properties such as the absorption (μ_a) and scattering (μ_s) coefficients, refractive index (ri) and anisotropic factor (g). Optical wavelengths of $660\,\mathrm{nm}$ (red, R) and $880\,\mathrm{nm}$ (infrared, IR), typically used for PPG acquisition, were simulated with the optical properties summarized in Table I. The neck tissue layers and optical properties were compiled from the relevant literature [5], [6], [7].

TABLE I: Optical properties of the neck tissue layers for wavelengths, red (R, $660\,\mathrm{nm}$) and infrared (IR, $880\,\mathrm{nm}$).

Tissue layers	$\mu_a(mm^{-1})$ R/IR	$\mu_s'(mm^{-1})$ R/IR	g R/IR	ri
Dermal	-	-	0.95	1.4
	-	-		
Fat	0.065	1.140	0.90	
	0.139	1.095		
Muscle	0.128	1.368	0.88	
	0.133	0.722	0.91	
Trachea	0	0	1	

The dermal layer was the perfused tissue layer. This was assumed to be a homogeneous mixture of dermal tissue and the main blood constituents, which are oxyhemoglobin (HbO_2) and deoxyhemoglobin (Hb). To incorporate dermal tissue-homogeneity into the model, the total absorption (μ_{a_D}) and total scattering (μ_{s_D}) coefficients with a blood volume fraction, V, at a given tissue oxygenation, S_tO_2, can be written as a cumulative coefficient ($\Sigma\mu_{k_D}$) using the following equation,

$$\Sigma\mu_{k_D} = (1-V)\mu_{k_{DB}} + \ldots \\ V\left[S_tO_2\mu_{k_{HbO_2}} + (1-S_tO_2)\mu_{k_{Hb}}\right], \quad (1)$$

where $\mu_{k_{DB}}$ can be either the absorption ($\mu_{a_{DB}}$) or reduced scattering ($\mu'_{s_{DB}}$) coefficients of a bloodless dermal layer. Similarly, $\mu_{k_{HbO_2}}$ and $\mu_{k_{Hb}}$ are the coefficient of oxy- and deoxy- hemoglobin, respectively. Simulations were carried out varying V at a fixed $95\,\%$ S_tO_2. The optical properties for blood, with a hematocrit (Hct) of $45\,\%$ were collected from published literature, and are summarized in Table II [8].

TABLE II: Optical properties in (mm^{-1}) for bloodless dermal (DB) and blood containing oxyhemoglobin (HbO_2) and deoxyhemoglbin (Hb) blood at each wavelength (λ), having $45\,\%$ hemotocrit (Hct).

λ (nm)	DB		HbO_2 $Hct = 0.45$		Hb $Hct = 0.45$	
	μ_a	μ_s	μ_a	μ_s	μ_a	μ_s
660	0.05	26.33	0.15	92.29	1.64	81.50
880		22.06	0.56	54.76	0.44	62.50

B. Monte Carlo modelling

The multilayer MC model has been explicitly described in earlier publications where the computational program was simulated in MATLAB®[1], [4]. A reflectance mode pulse oximetry geometry was modelled, where the source and detector were assumed to be placed in contact with the tissue surface. A Gaussian beam profile of $0.5\,\mathrm{mm}$ radius with R and IR wavelengths was considered, whilst the detector was defined with an active area of $1\,\mathrm{mm}^2$. Since wearable technologies have been reported to have source-detector separations (S-D) within $5\,\mathrm{mm}$ [9], simulations were performed until 10^6 photons were detected at separations between $2{-}6\,\mathrm{mm}$, with $0.2\,\mathrm{mm}$ increments.

To investigate the effects of S-D with the suprasternal notch tissue layers, the range of V within the dermal layer was varied between $2{-}10\,\%$, with $2\,\%$ increments. To understand the light-tissue interaction occurring at the suprasternal notch, investigations were carried out to observe the light-tissue interaction profile, mean optical path (MOP) and penetration depth (PD) for a given wavelength and S-D. Lastly, the mean detection efficiency (DE) was calculated by finding the ratio between the number of detected photons at a specific separation and the total photons simulated.

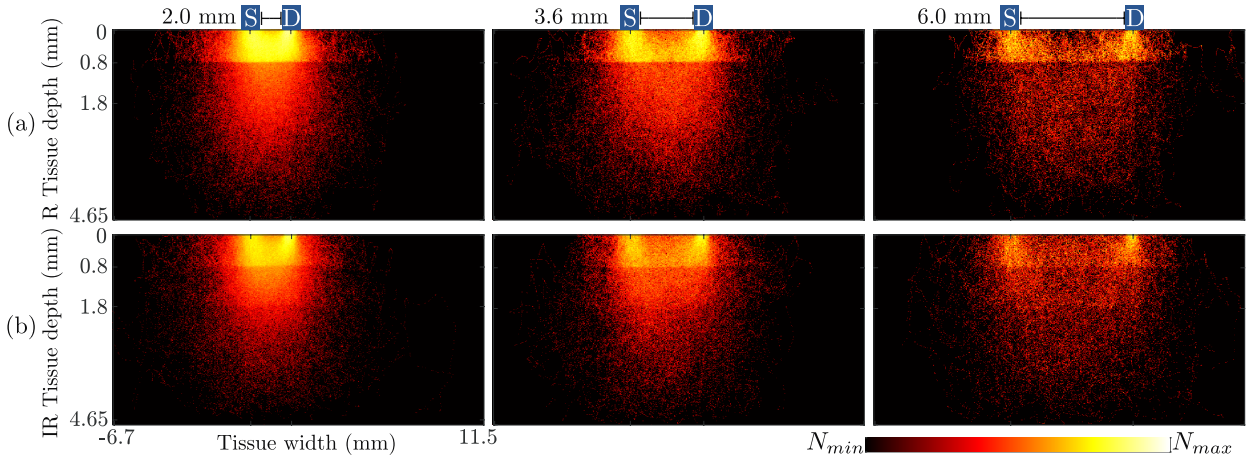

Fig. 2: Light-tissue interaction profiles in the neck model, between the source (S) and detector (D). The dermal layer contains 8% blood volume and 95% tissue oxygen saturation. The columns correspond to different source-detector separations, whilst the rows correspond to wavelengths, (a) red, R and (b) infrared, IR. The color bar represents the number of interactions, where black and white represents the minimum (N_{min}) and maximum (N_{max}) respectively. For better representation, the logarithm of data points have been taken. The range of tissue widths are all the same in all the graphs.

III. RESULTS

Fig 2 presents a 2D light-tissue interaction profile within the multilayer neck tissues at three source-detector separation (S-D) for wavelengths red (R) and infrared (IR). The maximum number of interactions (N_{max}) occurred near the source and detector whilst being confined within the dermal layer. The deeper the light penetrated, the smaller number of interactions. A clear boundary at a tissue depth of $0.8\,\mathrm{mm}$ can be observed between the dermal-fat layer, due to the scattering coefficient differences between the two layers. As the S-D increases for both wavelengths, the typical 'banana' shaped distribution of the scattered photons become more apparent.

In Fig 3, the mean penetration depth (PD) through the neck tissue at different separations for each wavelength is presented. The PD varies with wavelength and remains unchanged whilst V differs. For both wavelengths, as the S-D increases, the photons penetrate further into the tissue, although overall, photons at both wavelengths penetrate through similar tissue depths corresponding to the dermal-fat tissue boundary.

Fig 4(a-c) presents the simulated distributions of the mean optical pathlength (MOP) for S-D ranging between $2-6\,\mathrm{mm}$. As expected, the MOP travelled by both wavelengths increased with S-D and are not equal. R photons have a tendency to take a longer optical path compared to the IR photons. Furthermore, the difference between the R and IR MOP increased as S-D increased.

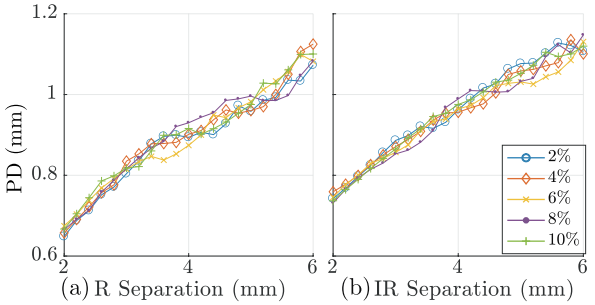

Fig. 3: Mean penetration depth (PD) whilst varying the source-detector separation and blood volume ($V, \%$). PD for wavelengths (a) red, R and (b) infrared, IR are presented.

Fig 4(d) presents the mean detection efficiency (DE) at each S-D combining all V. Both wavelengths show an exponential decay in the number of detected photons whilst the S-D increases. R has a lower DE compared to IR due to higher absorption coefficients in R.

Overall, the depth of penetration increased directly with the increasing S-D. For lower blood volumes, infrared photons penetrated deeper than red. As this was observed in a fixed tissue oxygenation, it is expected that the difference in PD for R and IR would change. The variation in the MOP and penetration depth were not identical, this indicating that a higher optical path does not translate to a higher penetration depth.

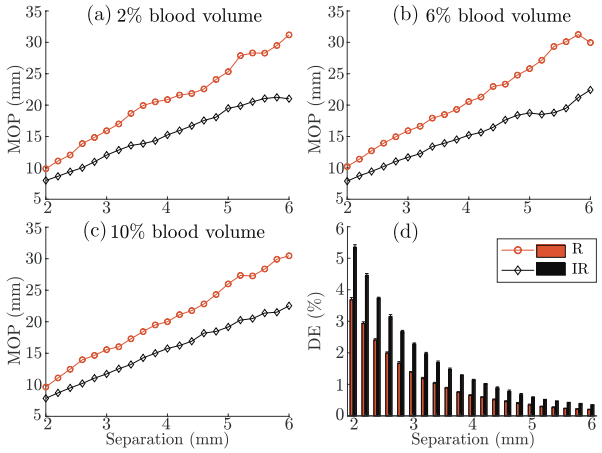

Fig. 4: Mean optical pathlength (MOP) and detection efficiency (DE) at red, R and infrared, IR. MOP at varying separations and blood volumes are presented in (a-c). DE for all blood volumes are presented in (d).

Since PPG originates from pulsatile arteries, the depth of these are an important factor for optimizing the S-D separation. The pulsatile blood manifests within the dermal layer of the suprasternal notch. Hence, ideally, the mean penetration depth should not exceed the dermal-fat boundary. Therefore, assuming a typical $0.8\,\mathrm{mm}$ the latter, when utilizing a wavelength of red and infrared, the sensor-detector separation should not exceed $3\,\mathrm{mm}$ and $2.4\,\mathrm{mm}$, respectively.

IV. Conclusion

In this paper, a 3D multilayer Monte Carlo model of light-tissue interaction in the suprasternal notch has been explored to characterize the interaction profile, optical pathlength, penetration depth and detection efficiency, for the first time. The model has been designed assuming a reflectance mode sensor, since this would be suitable for neck PPG acquisition. Anatomical parameters available from literature were carefully chosen to replicate the neck tissue as close as possible.

The effects on the optical pathlength and penetration depth with varying perfusion states and source-detector separation, for the chosen optical wavelengths, have been demonstrated. The variable perfusion state has been implemented in the model by altering the blood volume within the dermal layer of the neck. The investigations showed an overall reduction of detected light and increase in optical pathlength and penetration depth as the perfused blood volume increased.

When developing a wearable technology for neck PPG, determining the ideal distance between the source and detector, and understanding the region of light interrogation is important. When selecting an optimal separation distance, the PPG signal at both minimum and maximum perfusion variations should be detected. The simulation revealed that the optimal separation for red and infrared wavelengths, assuming typical anatomical parameters, are $3\,\mathrm{mm}$ and $2.4\,\mathrm{mm}$; since this would lead to closely interrogating the deep blood net plexus, the last dermal sublayer containing pulsatile blood [10]. Exceeding the optimal values would result in photons penetrating the subdermal fat and muscle, whilst reducing the detection efficiency. From the model, it can be seen that reducing the source and detector separation distance can improve the detection efficiency. However, care must be taken when reducing this distance as the chances of cross-talk between the source and detector would also increase. Larger separations might also be limited by the dimensions of the wearable.

This study represents a first attempt to model the light-tissue interaction in the neck. Further work should be carried out taking into account anatomical variations that would result in different values for the typical parameters used to extract the conclusions. This would include factors such as levels of melanin, skin hydration and body mass index.

References

[1] Z Patel *et al.*, "A Multilayer Monte Carlo Model for the Investigation of Optical Path and Penetration Depth at Different Perfusion States of the Colon," in *2019 41st Annual International Conference of the IEEE Engineering in Medicine and Biology Society (EMBC)*. jul 2019, pp. 3235–3238, IEEE.

[2] Y Sun *et al.*, "Photoplethysmography Revisited: From Contact to Noncontact, from Point to Imaging," *IEEE Transactions on Biomedical Engineering*, vol. 63, no. 3, pp. 463–477, 2016.

[3] I Garcia-Lopez *et al.*, "Characterization of Artifact Signals in Neck Photoplethysmography," *IEEE Transactions on Biomedical Engineering*, vol. 67, no. 10, pp. 2849–2861, 2020.

[4] S Chatterjee *et al.*, "In silico and in vivo investigations using an endocavitary photoplethysmography sensor for tissue viability monitoring," *J. Biomedical Optics*, vol. 25, no. 02, pp. 1, 2020.

[5] P Furlow *et al.*, "Surgical anatomy of the trachea," *Annals of Cardiothoracic Surgery*, vol. 7, no. 2, pp. 255–260, 2018.

[6] J Cheon *et al.*, "Ultrasonographic measurement of thickness of the thyrohyoid muscle: A pilot study," *Annals of Rehabilitation Medicine*, vol. 40, no. 5, pp. 878–884, 2016.

[7] A Bashkatov *et al.*, "Optical properties of human skin, subcutaneous and mucous tissues in the wavelength range from 400 to 2000 nm," *J. Phys. D: Appl. Phys*, vol. 38, 2005.

[8] N Bosschaart *et al.*, "A literature review and novel theoretical approach on the optical properties of whole blood," *Lasers in Medical Science*, vol. 29, no. 2, pp. 453–479, 2014.

[9] Ajmal *et al.*, "Monte Carlo analysis of optical heart rate sensors in commercial wearables: the effect of skin tone and obesity on the photoplethysmography (PPG) signal," *Biomedical Optics Express*, vol. 12, no. 12, pp. 7445, 2021.

[10] I Meglinski *et al.*, "Quantitative assessment of skin layers absorption and skin reflectance spectra simulation in the visible and near-infrared spectral regions," *Physiological Measurement*, vol. 23, pp. 741–753, 2002.